12-13-2023

The Analysis of Longitudinal Change Patterns in Developing Brain Using Functional and Structural Magnetic Resonance Imaging Data

Rekha Saha

Recommended Citation

Saha, Rekha, "The Analysis of Longitudinal Change Patterns in Developing Brain Using Functional and Structural Magnetic Resonance Imaging Data." Thesis, Georgia State University, 2023.
doi: https://doi.org/10.57709/36397807

The Analysis of Longitudinal Change Patterns in Developing Brain Using Functional and Structural Magnetic Resonance Imaging Data

by

Rekha Saha

Under the Direction of Vince D. Calhoun, Ph.D.

A Thesis Submitted in Partial Fulfillment of the Requirements for the Degree of

Master of Science

in the College of Arts and Sciences

Georgia State University

2023

ABSTRACT

This paper introduces a novel approach to explore longitudinal changes in brain functional network connectivity (FNC) and gray matter (GM) in adolescents, utilizing data from the Adolescent Brain and Cognitive Development (ABCD) study. The study focuses on multivariate patterns of FNC changes over a two-year period, identifying structured Functional Change Patterns (FCPs). One noteworthy finding is the strengthened functional connectivity between visual (VS) and sensorimotor (SM) domains as participants age. Moreover, the research highlights gender-specific variations in these patterns. This approach offers a robust means of assessing whole-brain functional changes longitudinally.

Additionally, the paper presents two complementary techniques for analyzing whole-brain structural and functional changes with age. The first method links Functional Change Patterns (FCPs) to voxel-wise ΔGM, revealing significant correlations for two components. The second technique investigates the connections between FCP and Structural Change Patterns (SCP). These methods provide valuable insights into the linked changes between functional connectivity and GM during adolescence, contributing to a comprehensive understanding of brain development.

INDEX WORDS: Delta FNC, Longitudinal study, ICA, MRI, Gray matter

The Analysis of Longitudinal Change Patterns in Developing Brain Using Functional and Structural Magnetic Resonance Imaging

by

Rekha Saha

Committee Chair:	Vince Calhoun
Committee:	Jingyu Liu
	Dong Hye Ye
	Murray Patterson

Electronic Version Approved:

Office of Graduate Services

College of Arts and Sciences

Georgia State University

December 2023

DEDICATION

I would like to dedicate this thesis to my family, friends, supervisor, and colleagues whose unwavering support and inspiration have been instrumental in guiding me on this journey and helping me reach my destination.

ACKNOWLEDGMENTS

I would like to thank Dr. Vince Calhoun, Dr. Jingyu Liu, Dr. Dong Hye Ye, and Dr. Murray Patterson for being the committee members of my thesis. I would like to give special thanks to Dr. Vince Calhoun for his continuous support and guidance to my MS journey. Finally, I would also like to give my special thanks to Debbrata Kumar Saha, my wonderful husband, for his endless love and support.

TABLE OF CONTENTS

LIST OF FIGURES

CHAPTER 1
LITERATURE REVIEWS

Human brain is considered as the most active organ which consumes about 20% of the energy from entire body - (Uludağ & Roebroeck 2014). Structural analysis shows that brain activities depend on different types of cells such as pyramidal neurons, interneurons, and glia. These cells distribution and connections between cells are developed via predetermined biological pathways. To analyze the complex structure of brain, there is a growing research interest in neuroimaging study. The ongoing research on Neuroimaging is playing vital role in different research fields, specially in the clinical diagnosis, and biomedical domains. The application of different neuroimaging technique has been grown rapidly in the past two decades. According to the imaging mode, neuroimaging technique is able to give both structural and functional images. Structural image can be used to visualize the structure of the brain for diagnosing the brain diseases like brain tumors or brain trauma. Functional image can be used to visualize how the brain metabolizes while carrying out certain tasks, including sensory, motor, and cognitive functions. Functional image is generally used in neuroscience and psychological research, but day by day it is going to be a new way to diagnosis clinical-neurology. Modern neuroimaging methods is able to reveal the relationship between the cognition and behavior in healthy subjects and its dysfunction in patients.

1.1 Magnetic Resonance Imaging (MRI) Basic

Neuroimaging can be considered as an umbrella for multiple methods, technologies, and modalities which is able to provide both structural and functional data regarding neu-

ral mechanisms. The most commonly used imaging technologies are magnetic resonance imaging (MRI), computerized tomography (CT), positron emission tomography (PET), and single-photon emission computed tomography (SPECT). Among them, Magnetic resonance imaging (MRI) is one of the widely used approaches in neuroimaging study. MRI has been utilized for demonstrating regional, time-varying changes in brain metabolism - (Bandettini et al. 1992; Kwong et al. 1992; Ogawa et al. 1990). Human brain used oxygen during metabolic activity; therefore, blood in the vicinity of metabolically active tissues will have a different proportion of oxygenated to deoxygenated hemoglobin (Hb) than that surrounding tissue - (Buxton et al. 1998; Davis et al. 1998). These two forms of Hb have different magnetic properties which creates the BOLD response. In the stimulated condition, increased blood flow causes the Hb to be swept out and replaced by HbO2, causing a BOLD signal increase. To capture these activities, MRI has been considered as one of the widely used tools. The MRI technique became popular as it is non-radioactive, non-invasive (does not require injection of a radioisotope or other pharmacologic agent), relatively low cost, and versatile. It has derived many unique imaging modalities, including diffusion-weighted imaging, diffusion tensor imaging, susceptibility-weighted imaging, and spectroscopic imaging. Each modality provides valuable and different types of information about brain structures and activity.

In MRI, there are two different approaches i) structural MRI, and ii) functional MRI to analyze the brain functionality. Structural MRI is used to analyze the brain morphometry. Meanwhile, functional MRI can be used to visualize how the brain metabolizes while carrying out certain tasks, including sensory, motor, and cognitive functions. Both structural

and functional MRI has been used extensively in neuroimaging study. In earlier studies, researchers considered functional and structural measures independently to analyze brain. But, recent studies are more focused to find the well-established links between the structural and functional neuronal level - (Chalfie et al. 1985; Gray et al. 2005). Recently, the practice to utilize the combined information of structural and functional MRI has been growing rapidly - (Rykhlevskaia et al. 2008).

1.2 Multimodal Fusion

Multimodal fusion is one of recently used neuroimaging techniques where it combines two or more data sets acquired from multiple imaging modalities and multiple techniques. This approach is mainly used to improve the understanding of the structure and function of the brain by utilizing complementary physical and physiological sensitivities. It also helps to overcome the fundamental limitations of individual modalities so as to understand brain dynamics with greater detail - (Calhoun & Sui 2016; Sui et al. 2014; Zhang et al. 2011). The main goal of multimodal fusion is to increase the strength of each modality in a joint analysis, rather than a separate analysis of each. However, despite improvements in individual modalities, it is becoming increasingly clear that the most effective research approaches will utilize multi-modal fusion, which takes advantage of the fact that each modality provides a limited view of the brain.

In neuroimaging studies, multimodal is a broadly used approach. The use of Multiple modalities from MRI data that has been collected from the same individual has been gaining

popularity day by day. Practically, it is proved that multimodal brain imaging studies are able to provide more complete understanding of the brain and its disorders, such as, it can provide information about how brain structure reflects the brain function, how brain are impacted by psychopathology and which functional or structural aspects of physiology could drive human behavior and cognition. Generally, there are 3 types of multimodal neuroimaging: (a) visual inspection: it is a unimodal analysis where results are visualized separately; (b) data integration: In data integration, obtained data from each unimodal technique are analyzed individually and then overlaid to prevents any interaction between different types of data - (Calhoun & Sui 2016) and (c) data fusion - (Sui et al. 2011) Data fusion can be categorized as asymmetric (one modality will constrain another modality) or symmetric (all modalities will be analyzed jointly). Each data fusion category uses a variety of techniques, including principal component analysis (PCA), independent component analysis (ICA), and general linear models.

1.3 Multivariate Methods for Multimodal Fusion

1.3.1 Joint ICA

In order to examine and analyze the shared information between the features found in the different imaging modalities, the joint analysis methods using the fusion technique is a must needed tool now a days. Joint ICA is one of the multivariate approaches which can be used to increase the covariation across datasets and maintains the high dimensionality in integrated modalities. Joint ICA is typically applied on two different imaging modalities and extracts

the spatially independent maps for each modality. Usually, these maps are coupled together by a shared loading parameter (the same mixing matrix). This approach has already been successfully used to combine different modalities such as fMRI-sMRI (GM) - (Calhoun et al. 2006b; Specht et al. 2008; Choi et al. 2008), fMRI-EEG - (Jorge et al. 2014; Calhoun et al. 2006a; Eichele et al. 2009; Calhoun et al. 2010), fMRI-DTI (FA) - (Franco et al. 2008; Teipel et al. 2010), GM-WM - (Xu et al. 2009). This provides a model-free approach to identify latent factors in complex datasets across vastly different data structures.

Joint ICA(JICA) fusion method has several advantages. Fusing data across modalities is important for disorders like schizophrenia where functional and structural deficits are widely reported, but the link between them has not yet been established fully. Thus, joint ICA is important to study the function/structure relationships of SZ patients. Second, Joint ICA shows a good spatial and temporal resolution in case of fusing fMRI, and EEG modalities together, and that is because fMRI has a good spatial resolution and EEG has a good temporal resolution.

1.3.2 Multimodal CCA

Multimodal CCA, as a technique, permits the use of distinct mixing matrices for each modality and aims to discover a transformed coordinate system that maximizes the covariance across two datasets - (Correa et al. 2008). This approach involves breaking down each dataset into a set of components, such as spatial areas in the case of fMRI/sMRI or temporal segments for EEG, along with their corresponding mixing profiles known as canonical variates (CVs). These CVs exhibit varying levels of activity among different subjects and

are considered linked when they exhibit similar modulation patterns across subjects. Following this decomposition, the CVs demonstrate correlations, but only for the same indices, and these correlations are referred to as canonical correlation coefficients (CCCs). In contrast to jICA, which enforces a shared mixing matrix for two or more features, mCCA offers more flexibility by permitting both common and distinct levels of connection between two features. However, it's important to note that the associated source maps may not exhibit spatial sparsity, especially when the CCCs are not distinct enough - (Correa et al. 2010a; Krol & Gimi 2020). Multimodal CCA is insensitive to variations in the data type ranges, making it suitable for jointly analyzing highly diverse data types. Furthermore, it can be expanded into multi-set CCA to accommodate more than two modalities - (Correa et al. 2010a; Li et al. 2009). It's worth mentioning that multimodal CCA operates on the second-level fMRI feature, specifically contrast maps. In contrast, multi-set CCA is capable of working with raw 4D fMRI data.

1.3.3 Linked ICA

Linked ICA is a probabilistic technique grounded in a modular Bayesian framework, developed to concurrently model and discover common features among various data modalities - (Groves et al. 2011). These combined modalities may exhibit distinct units, noise levels, spatial characteristics, and intensity distributions. Linked ICA offers two configurations: "linked tensor ICA" groups modalities from the same source with similar spatial properties, allowing them to share a common modality map. For example, FA, mean diffusivity (MD), and tensor mode (MO) can be configured as a tensor (DTI group data) to link GM. The

other configuration, "linked flat ICA," assigns each modality its own spatial map but shares the same subject-mixing matrix. In both scenarios, Bayesian tensor ICA - (Beckmann & Smith 2005) is employed to model each modality (group). This approach differs from traditional ICA methods like fastICA - (Oja & Hyvarinen 2000) and Infomax - (Bell & Sejnowski 1995) by incorporating dimensionality reduction directly into the ICA method through the use of automatic relevance determination (ARD) priors on components - (Bishop 1999) and by operating on the full-dimensional data.

1.3.4 mCCA+jICA

In the realm of brain connectivity studies that merge functional and structural aspects - (Rykhlevskaia et al. 2008; Camara et al. 2010), it is reasonable to hypothesize that components derived from each modality exhibit some level of correlation in their mixing profiles across subjects. The mCCA+jICA approach is a blind data-driven model specifically optimized for such a scenario - (Sui et al. 2011). It excels at achieving both flexible modal associations and source separation, making it a robust choice for handling various levels of modality connections. This approach leverages the strengths of two complementary techniques: mCCA and jICA. mCCA enhances the reliability of jICA by providing a closer initial alignment through correlation, while jICA further dissects the remaining mixtures within the associated maps and relaxes the requirement for distinct canonical correlation coefficients.

Importantly, the mCCA+jICA method does not significantly increase computational complexity. However, in simulations designed to mimic real-world brain imaging data fusion, it outperforms both mCCA and jICA when used in isolation. Furthermore, mCCA+jICA is

not limited to two-way fusion; it has the potential to extend to three-way or N-way fusion involving multiple data types. This can be achieved by substituting multimodal CCA with multi-set CCA - (Li et al. 2009). For instance, it can be applied to combine fMRI, sMRI, and genetic data to construct a comprehensive function-structure-genetics network, highlighting its broad applicability and potential widespread use.

1.3.5 Parallel ICA

The strict regularization enforced by the jICA framework can be relaxed in various ways to introduce more flexibility into the estimation process. One such approach is known as parallel ICA. This method serves as a framework for exploring data integration from two different imaging modalities, aiming to identify independent components in both modalities and establish connections between them by enhancing inherent interrelationships - (Liu & Calhoun 2007). The algorithm seeks to maximize the cost function, which considers both entropy and correlation terms. It proceeds by maximizing the independence of components within each data set separately. If the mixing profile correlations of certain components surpass a threshold, they are selected and employed to modify the demixing matrix update based on the correlation constraint, using suitable stopping criteria. It's important to note that the threshold is determined empirically and may vary for different combinations of data types. Due to its ability to enhance the inter-modality correlation of one or more components, parallel ICA is considered a semi-blind method. It has been applied to link fMRI with genetic data (specifically single nucleotide polymorphism arrays, SNP) - (Liu et al. 2009), as well as sMRI with SNP data - (Jagannathan et al. 2010). The results demonstrate that paraICA

yields stable outcomes and can accurately identify linked components with a relatively high level of precision - (Liu et al. 2008a).

1.3.6 CC-ICA

Coefficients-constrained ICA (CC-ICA) is designed to enhance the sensitivity of component extraction to detect group differences and improve decomposition accuracy. It's important to note that joint ICA is a blind method that does not incorporate prior diagnostic information and, therefore, is not optimized for identifying group differences. When the objective is to effectively identify potential disease biomarkers, incorporating prior membership information can significantly boost the method's sensitivity to detect relevant group differences. This led to the development of CC-ICA - (Sui et al. 2009b), which formulates the integration of a group difference criterion into the traditional ICA cost function. This adaptive constraint on the mixing coefficients of specific components serves to enhance the detection of group differences. CC-ICA can be combined with principal component analysis with reference (PCA-R) - (Caprihan et al. 2008; Liu et al. 2008b), providing a general approach for identifying disease biomarkers - (Sui et al. 2009a; Kim et al. 2010). One advantage of this approach is its ability to offer a unified and succinct representation of a particular group discriminative feature from multitask/multimodal data within a single component. CC-ICA can be applied to various multimodal combinations similar to joint ICA.

CHAPTER 2
WHOLE-BRAIN FUNCTIONAL NETWORK CHANGE PATTERNS

2.1 Introduction

The resting-state human brain can be used to reveal time-varying functional connectivity (FC) dynamics -(Chang & Glover 2010; Saha et al. 2020; Calhoun et al. 2014; Saha et al. 2019). There are various neuroimaging techniques that can be used to quantify FC. Functional magnetic resonance imaging (fMRI) is the most commonly used technique for the computation of the temporally coherent between brain blood oxygenation dependents. The FC between two brain regions from resting-state functional magnetic resonance imaging (rfMRI) data can be computed via a measure of pairwise statistical dependency (most commonly Pearlson correlation) between the time courses. Data-driven decomposition techniques such as independent component analysis (ICA) can be used to extract co-activated brain networks, whose time courses can be used to calculate the functional network connectivity (FNC) - (Jafri et al. 2008).

There is a growing research interest in estimating age-related anatomical and functional changes. Spontaneous blood oxygenation level-dependent (BOLD) signals have been frequently used to identify the regional FC and investigate the changes in a variety of neurological and psychiatric disorders - (Chen et al. 2011). During the adolescence period, the human brain exhibits remarkable changes both in function - (Vértes & Bullmore 2015; Stevens 2016) and structure - (Whitaker et al. 2016; Váša et al. 2018). Several studies have reported age-related FC changes during the adolescence period, but the obtained results are somewhat

inconsistent - (Váša et al. 2020). Small data size, the absence of longitudinal data, variation in fMRI data preprocessing, and the choice of different analysis methods contribute to this inconsistency. Vasa et al., have investigated changes in human brain function during adolescence and found two distinct modes (disruptive and conservative) of age-related change in FC. Age-related changes in FC have been studied including findings showing a progressive reduction in FC among different age groups - (Farras-Permanyer et al. 2019). The impact of aging on functional networks has also been reported in - (Geerligs et al. 2015). However, there has been little work in evaluating multivariate patterns of change in functional (network) connectivity with development.

In our work, we propose a new technique to visualize within-individual changes in whole-brain FNC with increased age. We estimate the FC change patterns (FCPs) by first computing cellwise within the individual ΔFNC matrix and then estimating covarying multivariate patterns via ICA on the ΔFNC matrices. A one-sample t-test on the resulting component loading parameters reveals several FCPs showing significant longitudinal differences. To the best of our knowledge, our proposed procedure is the first approach to estimate multiple overlapping brain functional change patterns (FCPs) over a two-year period in the developing brain. The remainder of the research paper is organized as follows. In the materials and methods section, we introduced the data preprocessing and the analysis procedures. Next, in the result section, we show brain functional coupling changes with age. Finally, we discuss the findings in the conclusion section.

2.2 Materials and Methods

2.2.1 Summary of ABCD data

The study utilized data from release 2.01 of the Adolescent Brain Cognitive Development (ABCD) study, accessible through its official website [1]. This dataset incorporates information from more than 11,800 children aged between 9 and 11 years, who underwent multiple MRI scans during two image sessions: the baseline and the second-year follow-up. The dataset includes a comprehensive collection of demographic and health-related information obtained with full written informed consent from the parents and assent from the children. These procedures were conducted under protocols approved by the Institutional Review Board (IRB). The ABCD dataset is shared through the National Institute of Mental Health Data Archive (NDA) website [2], which hosts open-source datasets sourced from various research endeavors spanning diverse scientific fields. This platform aims to facilitate collaborative scientific endeavors and enable exploration and discovery across multiple domains. For this study, data from 3,489 subjects who underwent scanning at both baseline and a two-year follow-up visit were utilized for analysis.

2.2.2 Data Preprocessing

The raw fMRI data underwent preprocessing using a combination of the FMRIB Software Library v6.0 (FSL) toolbox and the Statistical Parametric Mapping 12 (SPM) toolbox within the MATLAB 2019b environment. Initially, rigid body motion correction was applied us-

[1] https://abcdstudy.org/)
[2] https://nda.nih.gov/

ing FSL to rectify subject head motion. Subsequently, distortion in the fMRI images was corrected using field map files acquired with phase encoding in the anterior-posterior (AP) direction and volumes with phase encoding in the posterior-anterior (PA) direction. Following distortion correction, the fMRI data were standardized into the standard Montreal Neurological Institute (MNI) space with spatial resolutions set at $3 \times 3 \times 3$ and were then subjected to Gaussian smoothing with a full width at half maximum (FWHM) of 6 mm.

For this study, the Neuromark network templates were utilized to extract comparable Intrinsic Connectivity Networks (ICNs) through a fully automated spatially constrained ICA approach across subjects sourced from the ABCD dataset. The Neuromark framework employed two healthy control datasets, namely the Human Connectome Project (HCP) with 823 selected subjects and the Genomics Superstruct Project (GSP) with 1005 selected subjects, to construct the priors. More information regarding the Neuromark framework and templates can be found in - (Du et al. 2020). Additionally, research has shown that the selected spatial priors maintain high reliability across different pipelines and between datasets involving both adults and adolescents - (DeRamus et al. 2021).

2.2.3 Models

In our study, we worked with subject-specific Functional Network Connectivity (FNC) data obtained from both baseline and two-year scans. Initially, we computed cell-wise differences between the baseline and two-year FNC datasets, resulting in the creation of change matrices termed ΔFNCs. Subsequently, in pursuit of recognizing longitudinal brain functional coupling and capturing correlated patterns of alterations, referred to as Functional Change

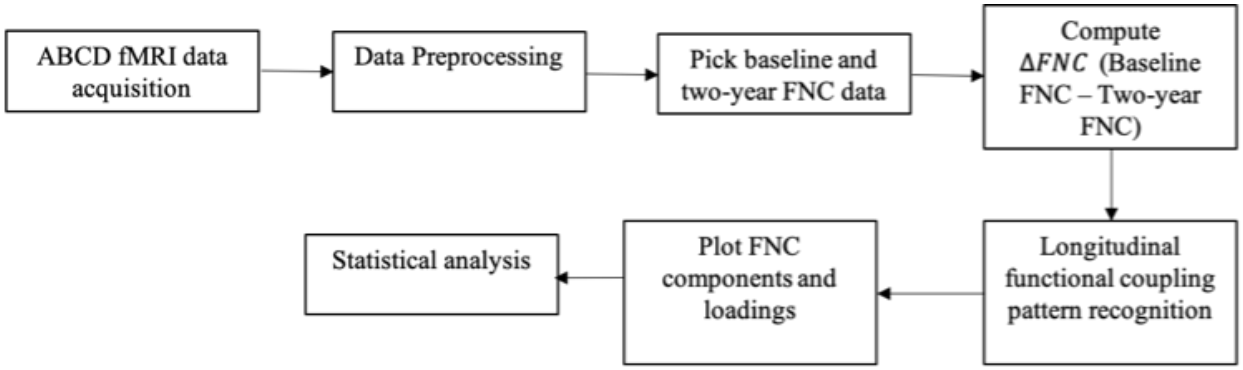

Figure 2.1: Block diagram of the FCP analysis workflow

Patterns (FCPs), we employed Independent Component Analysis (ICA) utilizing the infomax algorithm - (Bell & Sejnowski 1995) to decompose the ΔFNC matrices. In this particular experiment, we estimated 5 components through this decomposition. To illustrate, the model equation for the ICA can be expressed as:

$$X = A \cdot S \tag{2.1}$$

Here, X = Subjects (3489) × ΔFNC cells (1378 cells from the upper triangle of the symmetric matrix); A = subjects (3489) × component number (5) and S = component number (5) × ΔFNC cells (1378)

This effectively models the input data as:

$$\Delta FNC = \sum_{i=1}^{5} a_i FCP \tag{2.2}$$

Here, ΔFNC = F_0 - F_2, F_0 is the baseline FNC data, F_2 is the two-year FNC data, FCP, the source matrix, represents maximally independent functional change patterns, and

ai are the subject-specific loading parameters for each component. The sources represent maximally independent covarying patterns of functional change.

Following the ICA estimation, we proceeded to assess the loading parameters and source matrix to identify Functional Change Patterns (FCPs) exhibiting significant longitudinal changes in comparison to zero. This involved conducting one-sample t-tests on the loading parameters and determining their statistical significance at a 95% confidence level, corrected for multiple comparisons. Additionally, we created scatter plots of the loading parameters and generated spatial maps representing the Functional Network Connectivity (FNC) matrices. A graphical representation of this analysis workflow is depicted in Figure 2.1 within a block diagram format.

2.3 Results

The Neuromark template identified 53 replicable brain networks, which were subsequently grouped into 7 domains based on their anatomical and functional characteristics. These domains encompassed subcortical, auditory, sensorimotor, visual, cognitive control, default mode, and cerebellar networks (Du et al. 2020). Figure 2.2 visually presents the brain network template, with each color in the composite maps representing an intrinsic connectivity network in individual subplots

The experimental results for the Functional Connectivity Profiles (FCPs) are presented in Figure 2.3. This figure illustrates the 5 estimated components along with their associated T-values. The findings suggest a notable degree of modularity in the results, indicating

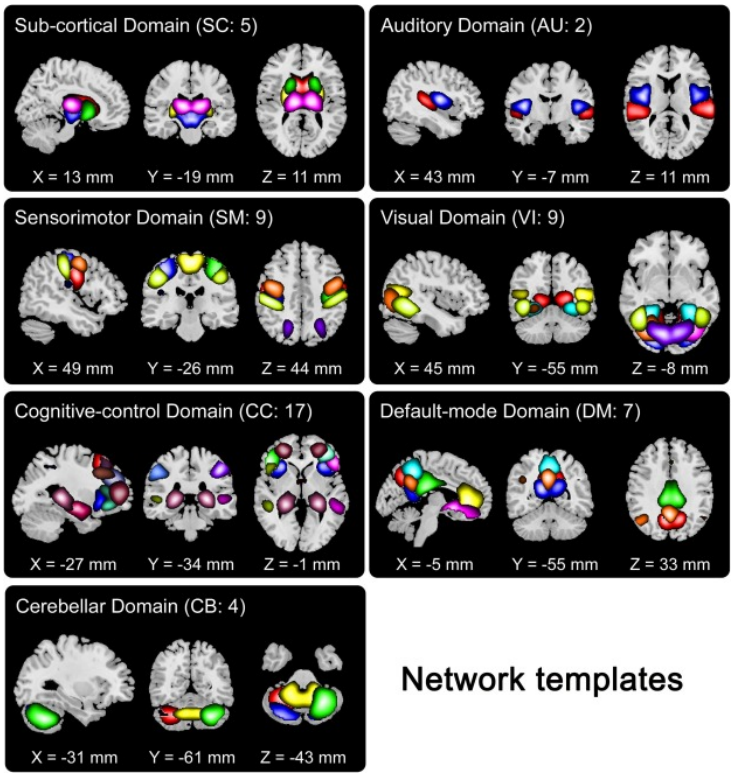

Figure 2.2: Visualization of Neuromark network template - (Du et al. 2020)

structured changes related to age. Notably, components 2 and 4 exhibit the highest positive and negative T-values, respectively. The T-values provide insights into the degree of expression of each FCP in the data, whether positively or negatively. A high negative (positive) T-value signifies an increased (decreased) expression of the respective FCP with age.

Specifically, Component 4 stands out with the most negative T-value of -14.02, indicating a strong negative expression in the data. In the plot, it's observed that the visual domain (VSN) - sensorimotor domain (SMN) and cerebellar domain (CBN) - subcortical domain (SCN) pairs display the most substantial negative values, suggesting increased brain functional coupling over a two-year span. Conversely, VSN-CBN and SMN-SCN domains exhibit decreasing change patterns with age.

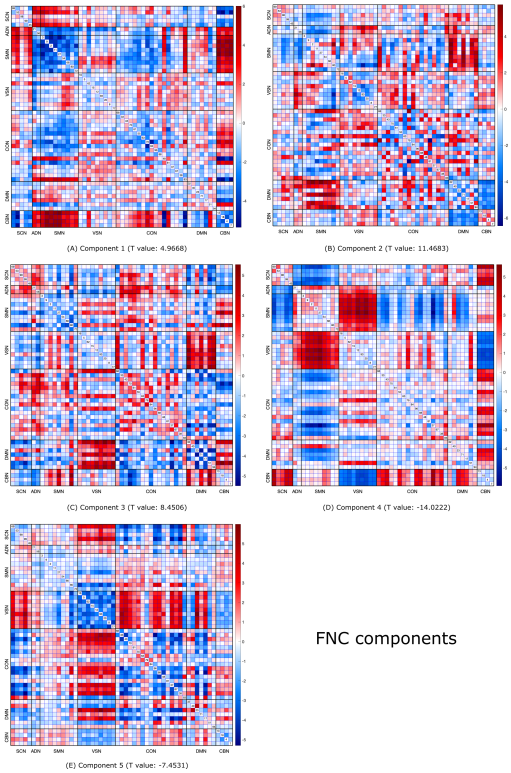

Figure 2.3: FNC component plot. In the figure, we observe the FCPs for components 2 and 4 have the highest positive (component 2) and negative (component 4) T-values.

For Component 2, there is a noticeable decrease in functional connectivity coupling between the default mode domain (DMN) and SMN as individuals age. The associated T-value for Component 2 is positive at 11.47, indicating a strong positive expression in the data. Additionally, increased functional coupling is observed between the CBN and DMN regions over the two-year period.

Loading scores were depicted using a raincloud plot, which provides a clear overview of the data distribution and its relationships through medians and confidence intervals. Figure 2.4 illustrates that Component 4 displays higher variance in loading parameters and a significantly negative mean value.

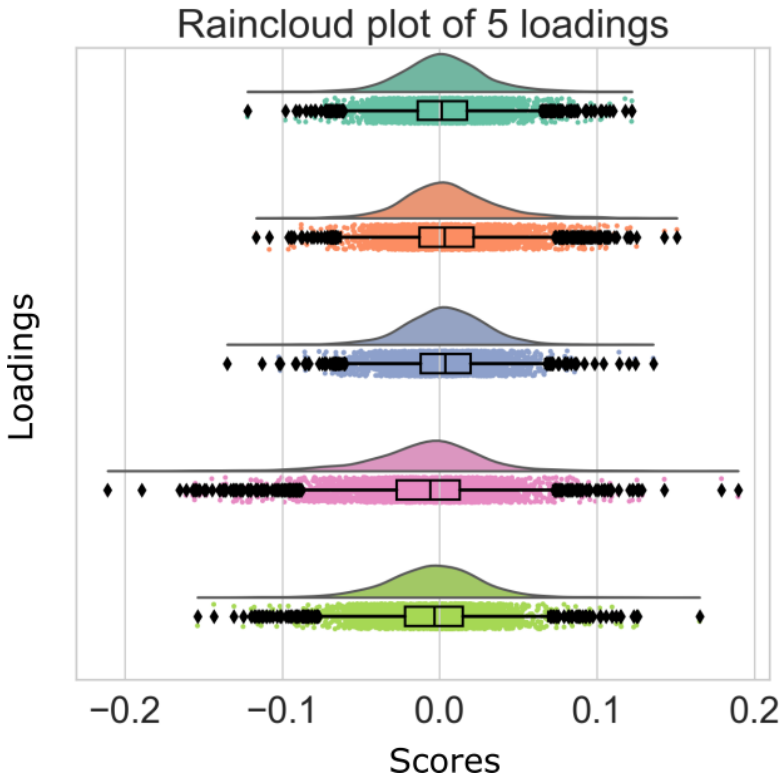

Figure 2.4: Scatter plot of loadings parameters. In the Y axis, we present five loadings and in the X axis, we present the scores of the corresponding loadings.

Finally, a two-sample t-test was conducted on each loading parameter based on sex information. The analysis revealed that males and females exhibit opposing effects on Components 4 and 5, with males showing smaller FCP changes for Component 4 and females showing smaller FCP changes for Component 5.

In summary, the study employed a template-based approach to identify consistent brain networks and investigated their relationships with age and gender, providing valuable insights into the functional connectivity profiles of these networks.

2.4 Discussion and Conclusion

In this research paper, we present an innovative method for analyzing multiple overlapping patterns of brain functional changes using Functional Network Connectivity (FNC) matrices. We specifically focus on the delta FNC matrix to illustrate alterations in brain functional connectivity associated with age. Our findings reveal several Functional Connectivity Patterns (FCPs) that exhibit significant changes over a two-year timeframe. Notably, we observe heightened functional connectivity between the Visual Network (VSN) and Sensorimotor Network (SMN) domains, alongside a reduction in anticorrelation between the Sensorimotor and Cognitive/Default Mode Network domains as individuals age. Furthermore, our investigation identifies both common and distinct patterns of brain functional changes in males and females. Specifically, males and females display adverse effects on components 4 and 5, but the direction of these effects differs between the genders. Our method holds promise as a robust tool for assessing comprehensive changes in brain function in longitudinal studies.

CHAPTER 3

FUNCTIONAL AND STRUCTURAL LONGITUDINAL CHANGE PATTERNS

3.1 Introduction

Magnetic resonance imaging (MRI) is one of the widely used approaches to capture brain structural and functional information from health control and patients - (Radua et al. 2014). Recently, Functional magnetic resonance imaging (fMRI) has been successfully utilized to compute the functional connectivity (FC) among different brain networks. FC can be quantified by spontaneous blood-oxygenation-level-dependent (BOLD) signal fluctuations between different brain regions obtained from resting-state functional magnetic resonance imaging (rfMRI) - (Fox & Raichle 2007). Functional connectivity is defined as the pairwise statistical dependency (most commonly Pearson correlation) between different brain areas - (Friston et al. 1993). Current studies have reported that functional connectivity between different brain regions changes during childhood and adolescence - (Fair et al. 2009; Kelly et al. 2009; Supekar et al. 2009; Thomason et al. 2008).

Recent studies are focused on finding the age-related anatomical and functional brain changes. The human brain experiences notable changes during adolescence, both in terms of function - (Stevens 2016; Vértes & Bullmore 2015) and structure - (Váša et al. 2018; Whitaker et al. 2016). Several studies have reported the connection between FC and structural connectivity (SC), such as the convergence of FC and SC in the default mode network (DMN) - (Greicius et al. 2009; Horn et al. 2014; Zhu et al. 2014), FC and SC properties vary

between groups, such as schizophrenic patients and controls - (Skudlarski et al. 2010; Zhou et al. 2008). There is a great deal of interest in understanding the brain by mapping its anatomical and functional connections. While some studies - (Andrews-Hanna et al. 2007; Betzel et al. 2014; Fjell et al. 2017b; Zimmermann et al. 2016) reported that age-related decline in functional connectivity is dependent on structural connectivity, some other studies found that structural connectivity only weakly restrains age-related changes in functional connectivity - (Fjell et al. 2017a; Tsang et al. 2017). However, there has been little work in estimating multivariate patterns of change in functional (network) connectivity and gray matter with increased age.

In this work, we propose two complementary approaches: 1) links between multivariate functional change patterns (FCPs) and voxel-wise gray matter (DGM) data and 2) multivariate change patterns (linking between FCP and structural change patterns (SCP)) to view within-individual alterations in whole-brain structure and function with increased age. In each individual, we calculate cell-wise DFNC and DGM matrix before estimating covarying multivariate patterns (FCPs) and (SCPs) via independent component analysis (ICA). Without a priori restrictions to particular seed regions, we computed the voxel-wise correlation between the loading parameters of functional data and DGM data. The second approach includes computing the correlation between the loading parameters of FC and GM data to visualize the relation between functional and structural change patterns. The remaining sections of this paper are structured as follows. In the method section, we will discuss the data preprocessing and workflow. Next, in the result section, we will present the obtained

results from functional and anatomical brain changes. Finally, we discuss our key findings in the conclusion section.

3.2 Materials and Methods

3.2.1 ABCD Data Summary

The investigation relied on the Adolescent Brain Cognitive Development (ABCD) study dataset, accessible via the official ABCD website [1]. The primary goal of the ABCD project is to track developmental changes in the human brain from childhood to adolescence. This trial involved approximately 11,800 children aged between 9 and 11, who underwent multiple MRI scanning sessions and provided health and demographic information. Access to the ABCD dataset is facilitated through the National Institute of Mental Health Data Archive (NDA) [2], which collates data from diverse research projects spanning various scientific domains. The NDA makes the ABCD dataset openly available to foster collaborative research endeavors and exploration. The fMRI data underwent preprocessing using a robust independent component analysis (ICA)-based framework called Neuromark, designed to identify brain networks by comparing data across subjects while accommodating individual variability within these networks - (Du et al. 2020). For this investigation, a subset comprising 2,734 participants with available baseline and two-year follow-up scans for both functional network connectivity (FNC) and gray matter data was utilized from this trial.

[1] https://abcdstudy.org/
[2] https://nda.nih.gov/

3.2.2 Preprocessing of fMRI Data

The data underwent preprocessing using a combination of the FMRIB Software Library v6.0 (FSL) toolbox and the Statistical Parametric Mapping 12 (SPM) toolbox within MATLAB 2019b. Initially, rigid body motion correction was applied using the FSL MCFLIRT tool to address subject head motion. Following this correction, distortion in the fMRI images was rectified using field map files obtained by capturing volumes with phase encoding in both the anterior-posterior (AP) and posterior-anterior (PA) directions using the FSL tool topup. The output field map coefficients obtained from the FSL tool applytopup were utilized to rectify the distortion in the fMRI volume. Subsequently, the fMRI data underwent Gaussian smoothing with a full width at half maximum (FWHM) of 6 mm and were warped to the standard Montreal Neurological Institute (MNI) space with spatial resolutions of $3 \times 3 \times 3$.

For the analysis, a fully automated spatially constrained Independent Component Analysis (ICA) technique was employed to extract intrinsic connectivity networks (ICNs) and their corresponding time courses (TCS) across subjects from the ABCD dataset. This extraction was facilitated using the Neuromark network templates, derived from replicated networks obtained from two datasets of healthy controls: the Human Connectome Project (HCP) consisting of 823 individuals post-subject selection and the Genomics Super Struct Project (GSP) comprising 1005 subjects post-subject selection. Further information about the Neuromark templates can be found at [3] and within the GIFT toolbox - (Du et al. 2020). Notably, studies have demonstrated that the chosen spatial priors exhibit high reliability

[3] http://trendscenter.org/data

across pipelines, datasets encompassing both adults and adolescents, and diverse populations, while also accounting for individual subject variability - (DeRamus et al. 2021).

3.2.3 Preprocessing of sMRI Data

The sMRI data underwent preprocessing utilizing statistical parametric mapping (SPM12[4]) within the MATLAB 2020b environment. The initial step involved segmenting the structural images into distinct components such as gray matter, white matter, and cerebrospinal fluid (CSF), while also incorporating modulation by the Jacobian. This segmentation process resulted in voxel-wise maps representing gray matter volume (GMV). Subsequently, the GMV maps underwent a smoothing procedure using a Gaussian kernel with a full width at half maximum (FWHM) set at 6 mm.

3.2.4 Models

In our investigation, we utilized subject-specific fMRI and sMRI data obtained from both baseline and two-year scans. To generate altered Functional Network Connectivity (FNC) and Gray Matter (GM) matrices, we initially computed cell-wise differences between the baseline and two-year FNC and GM data. Subsequently, employing Independent Component Analysis (ICA) using the infomax technique - (Bell & Sejnowski 1995), we decomposed the ΔFNC and ΔGM matrices. This allowed us to capture correlated patterns of change termed as Functional Change Patterns (FCPs) and Structural Change Patterns (SCPs). These patterns aimed to recognize the longitudinal coupling between brain function and structure.

[4]http://www.fil.ion.ucl.ac.uk/spm/

In our experiment, we estimated thirty components for GM data and five components for the FNC data, determined based on the elbow criteria. Specifically, the equation for this secondary-level ICA model can be expressed as:

$$X = A \cdot S \tag{3.1}$$

Here, the dimensionality of the data matrix X is 2734 (subjects) $\times$ cells (for fMRI, the upper triangle elements of the ΔFNC matrix; for sMRI, the number of voxels). Also, A is 2734 $\times$ components and S is components $\times$ cells.

This effectively models the functional input data as:

$$\Delta FNC = \sum_{i=1}^{5} a_i FCP \tag{3.2}$$

$$\Delta GM = \sum_{i=1}^{5} a_i SCP \tag{3.3}$$

Here, ΔFNC=F_0 -F_2 and ΔGM=G_0 -G_2, where F_0 and F_2 are the baseline and two-year FNC data, G_0 and G_2 represent the baseline and two-year GM data respectively. FCP and SCP are the source matrix, reflecting functional change patterns and structural change patterns respectively with the greatest degree of independence, and a_i and b_j are each component's subject- specific loading parameters of FNC and GM data respectively. The sources for FNC and GM data depict FCPs and SCPs, respectively, that are optimally independent and covarying.

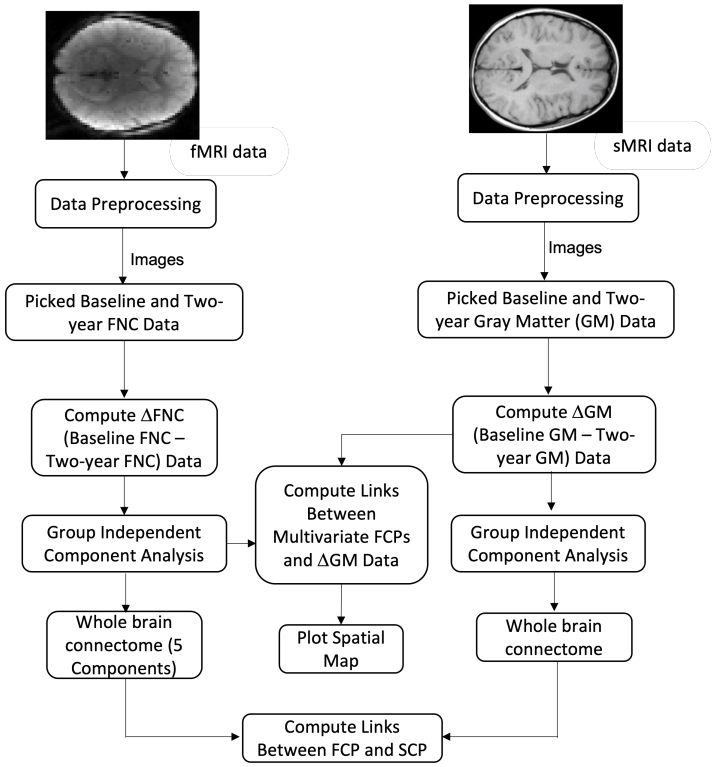

Figure 3.1: Block diagram of the functional and structural change patterns analysis workflow

We pursued two distinct methods to uncover the relationship between functional and structural changes, aiming to identify their respective change patterns. Firstly, one approach involved computing voxel-wise correlations between the ΔGM data and the loading parameters obtained from the ICA estimation of functional data. This allowed us to scrutinize the covariation of functional change patterns across the loading parameters of each component. Secondly, employing a different strategy, we conducted statistical analyses to ascertain the connection between the loading parameters derived from altered functional and GM data. Additionally, we visualized the Structural Change Patterns (SCPs) of GM data through spatial maps for components 1, 2, 4, and 26. A graphical representation of the analysis workflow is illustrated in Figure 3.1.

3.3 Results

The experimental results, as illustrated in Figure 3.2, display spatial maps indicating the relationships between multivariate Functional Connectivity Patterns (FCPs) and voxel-wise Gray Matter (GM) data. In this figure, five FCP components are plotted alongside spatial maps depicting the correlations between GM data and FCP loadings, with a focus on their associations with increasing age. The findings suggest substantial connections between FCPs and voxel-wise GM data. Additionally, the co-variation between the loading parameters was explored, revealing a correlation value of -0.38 between loadings 4 and 2 of FCPs. The spatial map figure shows that component 2 is significantly positively correlated, while the sub-cortical domain (SCN) exhibits a widespread negative correlation with altered GM data. Notably, the voxel-wise correlation map indicates that components 2 and 4 of FCP exhibit similar correlations with altered GM data, but with opposite directions.

Furthermore, a strong positive correlation ($r = 0.35$) is observed between loadings 4 and 5 of FCPs. Similar to component 4, the voxel-wise correlation map shows a significant negative correlation between FCPs and voxel-wise altered GM data for component 5. Conversely, the SCN exhibits a significant positive correlation, displaying notable differences in the sub-cortical region in the voxel-wise correlation between components 2 and 4, with component 4 exhibiting a higher voxel-wise correlation in the SCN.

After performing Independent Component Analysis (ICA) on each modality, we calculated Pearson correlations between the loading parameters of altered functional and GM data to identify links between the FCPs and Structural Connectivity Patterns (SCPs). Figure 3.3

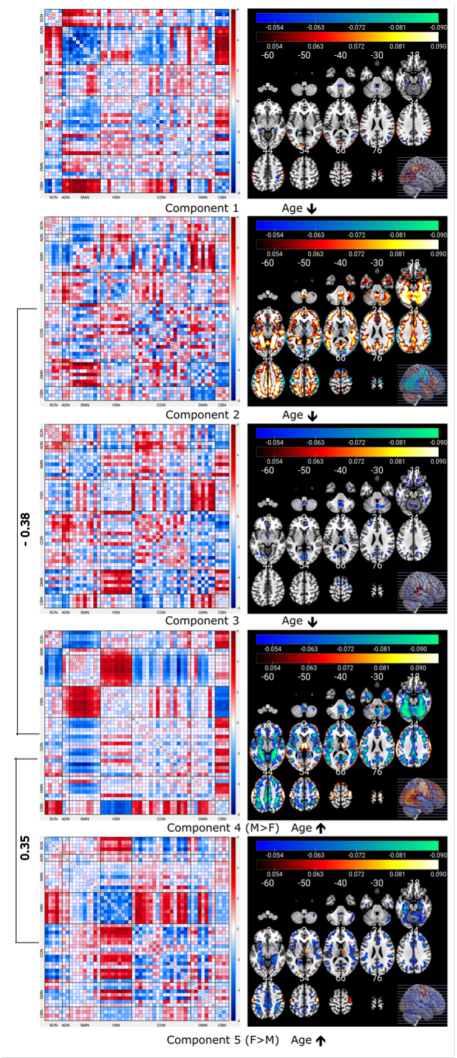

Figure 3.2: FNC component plot and spatial map of voxel-wise GMV correlation with the FCP loading parameters for each component. In the figure, we observe the voxel-wise correlation for components 2 and 4 have the highest positive (component 2) and negative (component 4) values.

illustrates the connections between multivariate change patterns. Some SCP components, specifically 1, 2, 4, and 26, are associated with FCP components. Notably, component 1 (r = 0.055, p = 0.0040) and component 2 (r = -0.06, p = 0.0017) of GM data are correlated with component 1 of Functional Network Connectivity (FNC) data. Additionally, component 4 (r = -0.052, p = 0.0065) and component 26 (r = 0.053, p = 0.0056) of GM data are correlated

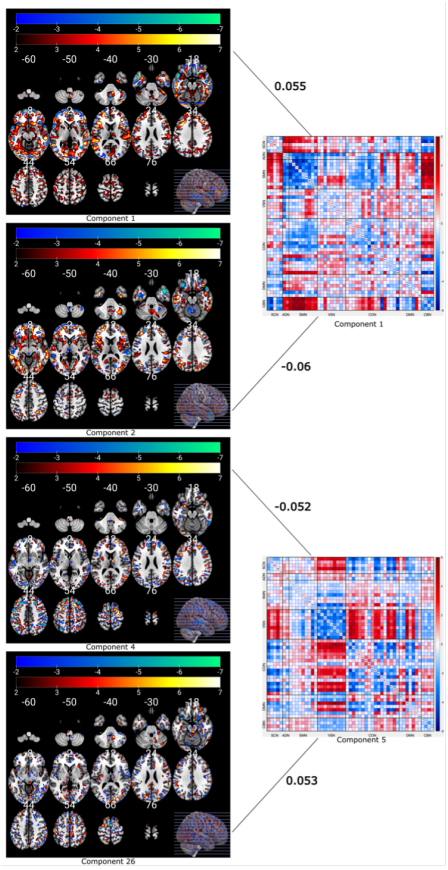

Figure 3.3: Spatial maps of gray matter data for components 1, 2, 4, and 26. Components 1 and 2 of SCP are linked with component 1 of FCP and components 4 and 26 of SCP are linked with component 5 of FCP.

with component 5 of FNC data. Based on these correlation values, it can be concluded that there is an association between FCP and SCP. Furthermore, by considering gender information, a two-sample t-test was conducted on the loading parameters of components 1, 2, 4, and 26 of GM data. The analysis reveals that males exhibit smaller SCP changes for component 2, while females exhibit smaller SCP changes for component 1.

3.4 Discussion and Conclusions

In this paper, we introduce two complementary methods aimed at exploring comprehensive whole-brain structural and functional changes, as well as their relationships with the aging process. We leverage functional and gray matter data from the ABCD study to analyze our models. The first method involves establishing links between Functional Connectivity Patterns (FCP) and "raw" voxel-wise gray matter (GM) data. The second method explores the connections between FCP and Structural Connectivity Patterns (SCP) by examining their loadings. Our objective is to gain insights into the trends associated with aging. When analyzing FCP components 2 and 4, we observe a widespread correlation between their loadings and voxel-wise GM data. Furthermore, we identify connections between FCP and SCP loadings for certain components, leading us to hypothesize that multivariate patterns of functional network connectivity (FNC) and gray matter (GM) exhibit associations with age-related changes. Additionally, we conducted a two-sample t-test on the loading parameters of GM data, considering gender information. Our analysis reveals that males demonstrate fewer significant SCP changes for component 2, while females exhibit fewer significant SCP changes for component 1.

CHAPTER 4

MULTIMODAL FUSION OF FUNCTIONAL AND STRUCTURAL DATA TO RECOGNIZE LONGITUDINAL CHANGE PATTERNS

4.1 Introduction

Magnetic resonance imaging (MRI) is a widely utilized method for acquiring valuable brain information and one of the only modalities that can visualize brain structure and function. Structural neuroimaging modalities, such as structural MRI (sMRI) and diffusion MRI (dMRI), provide insights into the anatomical structure and tissue composition of the brain. In contrast, functional neuroimaging modalities, such as fMRI based on blood-oxygenation-level-dependent (BOLD) signal, indirectly measure brain function and activity - (Abrol et al. 2017; Ogawa et al. 1990). Previous studies have predominantly examined functional and structural measures independently when analyzing the brain. However, there has been a rapid increase in the utilization of combined structural and functional MRI data - (Rykhlevskaia et al. 2008). Multimodal fusion of neuroimaging data is a technique that integrates data acquired from multiple imaging modalities and techniques. This approach aims to overcome the inherent limitations of individual modalities and gain a deeper understanding of brain dynamics - (Calhoun & Sui 2016; Sui et al. 2014; Zhang et al. 2011). The primary objective of multimodal fusion is to enhance the analytical power of each modality through joint analysis, rather than separate analyses of each modality.

In order to analyze the shared information among the features found in different imaging modalities, we used multiset canonical correlation analysis + joint independent component

analysis (mCCA+jICA) method, a widely recognized and extensively used multimodal fusion approach - (Sui et al. 2011). mCCA+jICA, is a data-driven multivariate fusion technique - (Correa et al. 2010b; Calhoun et al. 2006b) that simultaneously analyzes multimodal data by combining mCCA and jICA in a two-step process - (Calhoun & Sui 2016). In the first step, mCCA is utilized to identify highly correlated components between multiple modalities - (Sui et al. 2011, 2013). This is followed by the application of jICA in the second step to decompose these correlated components into spatially independent components, known as ICs. The mCCA+jICA algorithm has been employed - (Sui et al. 2011) to combine fMRI contrast maps and diffusion tensor imaging (DTI) fractional anisotropy (FA) maps for examining group differences among healthy controls (HCs), schizophrenia patients (SPs), and bipolar patients (BPs). Importantly, that study found that the combined algorithm yielded increased accuracy in group classification compared to using the constituent algorithms individually. Ouyang et al. have used the mCCA+jICA approach to identify patterns of gray matter (GM) and white matter (WM) covariance in patients with Alzheimer's disease - (Ouyang et al. 2015). Similarly, Kim et al. utilized mCCA+jICA with multimodal sMRI and DTI data from patients with obsessive-compulsive disorder and HCs, revealing significant alterations in the interconnected networks of GM and WM - (Kim et al. 2015). But, to the best of our knowledge, no previous studies have been conducted to estimate the changes in sex-related multivariate patterns coupling in FNC and GM associated with age progression using the mCCA+jICA multimodal fusion analysis method.

In this study, we propose a novel approach to investigate the relationship between within

subject age-related changes in whole-brain structure and function at an individual level. For each participant, we calculate cell-wise differences (ΔFNC and ΔGM) and then estimate covarying multivariate patterns (functional change patterns (FCPs) and structural change patterns (SCPs)) using the mCCA+jICA multimodal fusion method. By performing a one-sample t-test on the loading parameters of the resulting multimodal components, we identify several FCPs and SCPs that exhibit significant longitudinal differences. Furthermore, we explore the interaction between functional and structural changes in both males and females. The rest of this paper is structured as follows: the method section describes the data preprocessing steps, workflow, and analysis procedures. In the results section, we present the findings related to functional and anatomical brain changes associated with age. Lastly, we discuss the significant implications of our findings in the conclusion section.

4.2 Materials and Methods

4.2.1 Adolescent Brain Cognitive(ABCD) Data Summary

This investigation utilized the dataset derived from the Adolescent Brain Cognitive Development (ABCD) study, available through the official ABCD website [1]. The primary aim of the ABCD project was to track changes in the human brain as individuals transition from childhood to adolescence. It involved more than 11,800 children, aged 9 to 10 at the baseline session, who underwent multiple MRI scans. Alongside MRI scans, their health and demographic information was collected. The ABCD dataset is accessible through the National

[1] https://abcdstudy.org/

Institute of Mental Health Data Archive (NDA) website [2]. The NDA serves as a repository for data from various research initiatives across different scientific fields and provides the ABCD data as an open-source dataset, promoting collaborative research and investigation. To ensure data quality, the fMRI data underwent preprocessing using a robust independent component analysis (ICA)-based framework called Neuromark. This framework compares data across individuals to identify brain networks while accommodating variations unique to each individual within the networks - (Du et al. 2020). For this study, a subset consisting of 2,734 participants who had both baseline and two-year follow-up scanned data available for both functional network connectivity (FNC) and gray matter volume was selected for analysis.

4.2.2 Preprocessing of fMRI Data and Functional Feature Extraction

The data preprocessing involved a combination of tools: the FMRIB Software Library v6.0 (FSL) toolbox and the Statistical Parametric Mapping 12 (SPM) toolbox within MATLAB 2020b. To correct for subject head motion, the FSL MCFLIRT tool was utilized for rigid body motion correction. Subsequently, distortion in the fMRI images was addressed using field map files. These field maps were generated by acquiring volumes with phase encoding in both anterior-posterior (AP) and posterior-anterior (PA) directions using the FSL tool topup. By leveraging the output field map coefficients from the FSL tool applytopup, distortion in the fMRI volume was rectified. The fMRI data underwent smoothing with a Gaussian kernel of full width at half maximum (FWHM) set to 6 mm and were then transformed

[2]https://nda.nih.gov/

to the standard Montreal Neurological Institute (MNI) space with a spatial resolution of $3 \times 3 \times 3$.

After preprocessing, a fully automated spatially constrained Independent Component Analysis (ICA) method was employed to extract intrinsic connectivity networks (ICNs) and their corresponding time courses (TCS) from the ABCD dataset. This extraction was facilitated using the Neuromark_fMRI_1.0 template -(Du et al. 2020). This template was created by aggregating replicated networks from two datasets: the Human Connectome Project (HCP) dataset comprising 823 selected individuals and the Genomics Super Struct Project (GSP) dataset comprising 1005 selected subjects. More comprehensive details about the Neuromark template can be found on the website [3] and within the GIFT toolbox. Notably, the selected spatial priors have demonstrated high reliability across various pipelines, datasets inclusive of both adults and adolescents, and diverse populations - (DeRamus et al. 2021).

4.2.3 Preprocessing of sMRI Data

The sMRI data underwent preprocessing using the Statistical Parametric Mapping (SPM12[4]) software, operated within the MATLAB 2020b environment. Initially, the structural images underwent segmentation to distinguish between gray matter, white matter, and cerebrospinal fluid (CSF). This segmentation process also involved modulation by the Jacobian, resulting in voxel-wise maps of gray matter volume (GMV). Following this, the GMV maps underwent a smoothing procedure using a Gaussian kernel with a full width at half maximum (FWHM)

[3] http://trendscenter.org/data
[4] http://www.fil.ion.ucl.ac.uk/spm/

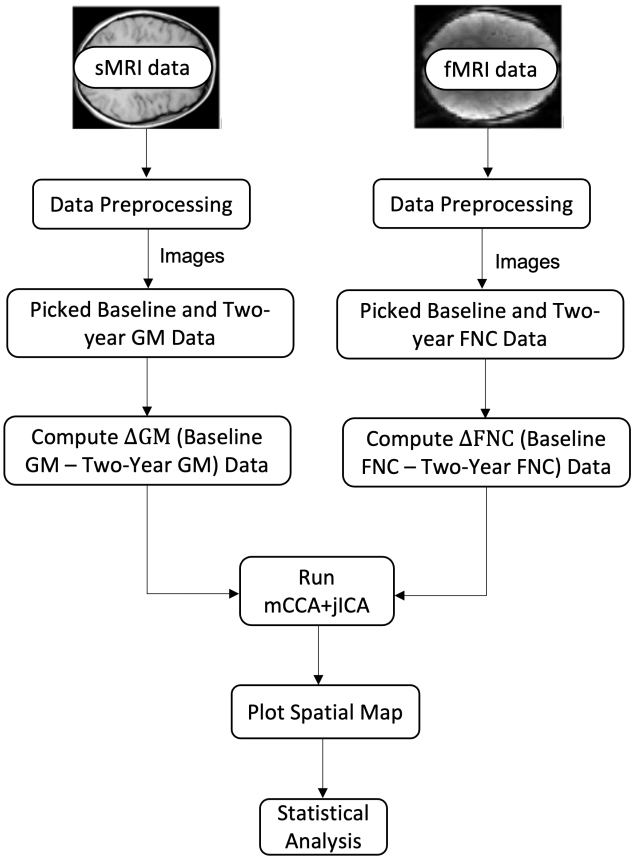

Figure 4.1: Block diagram of the functional and structural change patterns recognition workflow

of 6 mm. This smoothing step aimed to improve the spatial smoothness of the data.

4.2.4 Models

In our study, we worked with subject-specific fMRI and sMRI data collected at both baseline and two-year scans. To understand alterations in functional network connectivity (FNC) and gray matter (GM), we computed the differences between the baseline and two-year data for each cell. These matrices of differences, labeled as ΔFNC and ΔGM, represented changes in FNC and GM over the given timeframe. Subsequently, we applied the mCCA+jICA

method to break down the ΔFNC and ΔGM matrices. This method enabled the extraction of correlated change patterns: functional change patterns (FCPs) and structural change patterns (SCPs), respectively. To achieve this, we derived five components for both GM and FNC data, determining the optimal number of components using the elbow criterion. The mCCA+jICA model equation utilized in our study is outlined below:

$$X_k = A_k \cdot S_k \tag{4.1}$$

In this equation, the dimensionality of the data matrix X is 2734 (subjects) × cells (for fMRI, the upper triangular elements of the ΔFNC matrix; for sMRI, the number of voxels). The dimensions of A are 2734 × 5 (components), S is 5 (components) × cells, and k = 2 is the number of modalities.

This effectively models the input data as following :

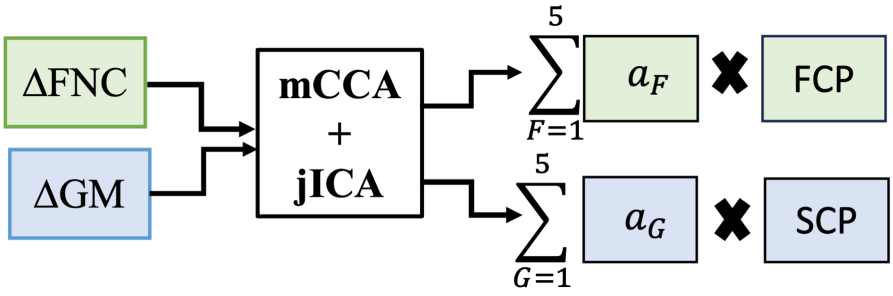

Here, ΔFNC represents the difference between the baseline (F_0) and two-year (F_2) functional network connectivity (FNC) data, while ΔGM corresponds to the difference between the baseline (G_0) and two-year (G_2) gray matter (GM) data. The FCPs and SCPs source matrices capture the most independent patterns of functional and structural changes, respectively. The terms a_F and a_G refer to the subject-specific loading parameters for each

component in the FNC and GM data, respectively. These loading parameters quantify the contribution of each subject to the respective components.

Following the mCCA+jICA estimation, we analyzed the loading parameters and source matrix. To identify significant longitudinal changes in Functional Connectivity Patterns (FCPs) and Structural Connectivity Patterns (SCPs), one-sample t-tests were conducted on both modalities' loading parameters (a_F and a_G). We ensured a statistical significance level of 95%, adjusted for multiple comparisons. Furthermore, we segregated the GM and FNC data by gender and computed correlations between male and female loadings in each modality. Assessing the difference between these correlations (female - male) allowed us to gauge the gender-related strength of coupling between GM and FNC loadings. A notably positive difference would imply a stronger GM-FNC coupling in females compared to males. A graphical representation of the analysis workflow is illustrated in Figure 4.1.

4.3 Results

The Neuromark template encompasses a total of 53 replicable networks, classified into 7 domains based on anatomical and functional features: subcortical, auditory, sensorimotor, visual, cognitive control, default mode, and cerebellar domains - (DeRamus et al. 2021). The experimental outcomes are presented in Figure 4.2, which features spatial maps illustrating the connections between multivariate Functional Connectivity Patterns (FCPs) and Structural Connectivity Patterns (SCPs). This figure showcases 5 components of FCPs alongside corresponding spatial maps of SCPs components, with associated T-values indicating the

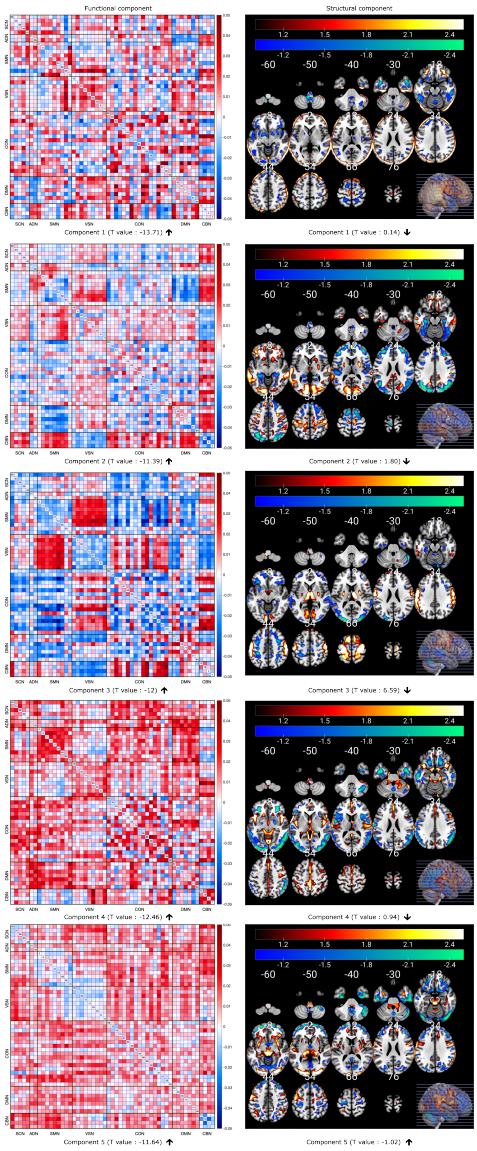

Figure 4.2: FNC components and spatial map of GM components. Here, Component 3 from both functional and structural data exhibits highly structured changed patterns.

degree of expression change with age - (Saha et al. 2022). The upper and lower arrows represent increasing and decreasing patterns with age, respectively. The results unveil notable modularity, indicating structured changes occurring over the two-year period.

Components 2 and 3 of functional connectivity patterns (FCPs) exhibit significant changes

with age in the developing brain. Both components show an increasing trend with age, as indicated by their negative T-values. Component 3 reveals increased brain functional connectivity between the visual domain (VS) and sensorimotor domain (SM) in the Functional Network Connectivity (FNC) data. Correspondingly, there are decreasing changes in the bilateral sensorimotor cortex in the structural MRI (sMRI) data over the two-year period. Additionally, FCP component 3 shows a decreasing trend with age in the functional connectivity between the VS and cerebellar domain (CB), as well as between the SM and cognitive control domain (CO).

Following the multimodal fusion technique, Pearson correlation was calculated between the loading parameters across all FCPs and SCPs, separately for males and females. The aim was to investigate gender differences in coupling (subject expression-level associations). The analysis revealed that females exhibited stronger coupling between SCP component 2 and FCP component 1 (Δr = 0.128, FDR-corrected, P = $2.1895e^{-11}$), FCP component 3 (Δr = 0.102, FDR-corrected, P = $1.0081e^{-07}$), and FCP component 4 (Δr = 0.111, FDR-corrected, P = $6.7136e^{-09}$) compared to males. This finding suggests that females, contributing the most to the structural change pattern (SCP component 2), also significantly contribute to FCPs components 1, 3, and 4. Based on the obtained correlation values, it can be concluded that females exhibit stronger coupling between FCPs and SCPs expressions compared to males. Additionally, a two-sample t-test based on gender information using the loading parameters of both modalities revealed that males exhibit smaller change pattern expression in SCP for component 2 compared to females.

4.4 Discussion and Conclusions

This paper introduces an innovative approach to explore the intricate relationship between multivariate brain functional and structural change patterns by leveraging Functional Network Connectivity (FNC) matrices and Gray Matter (GM) data. The main objectives of this research involve the investigation of comprehensive structural and functional changes across the entire brain over a span of two years, the examination of age-related trends in these alterations, and the analysis of the interplay between structural and functional changes with consideration to gender differences. The study employs functional and GM data sourced from the ABCD dataset. The results highlight significant changes in various Functional Connectivity Patterns (FCPs) and Structural Connectivity Patterns (SCPs) over the specified two-year duration. Additionally, the study uncovers that females exhibit a more pronounced coupling between functional change patterns (specifically, components 1, 3, and 4) and structural change patterns (component 2) when compared to males. These findings underscore the potential of the proposed approach as a valuable tool for assessing comprehensive functional and structural changes across the entire brain, along with their interconnections, in longitudinal studies involving both male and female subjects.

CHAPTER 5
CONCLUSIONS AND FUTURE WORK

This paper introduces a novel approach for analyzing multiple overlapping brain functional change patterns using FNC matrices, specifically focusing on age-related brain functional connectivity changes. The findings indicate the existence of significant changes in several Functional Change Patterns (FCPs) over a two-year period. These changes involve heightened functional connectivity coupling between the Visual-Salience Network (VSN) and Sensorimotor Network (SMN) domains and a reduced anticorrelation between the sensorimotor and cognitive/default mode network domains as age increases. Moreover, it unveils gender-specific brain functional pattern changes, with males and females exhibiting contrasting effects on components 4 and 5. This approach shows great potential as a robust tool for evaluating comprehensive whole-brain functional changes in longitudinal studies.

In addition, this paper presents two complementary methods: the connection between FCP and voxel-wise Gray Matter (GM) and the relationship between FCP and Structural Change Patterns (SCP) via their loadings. These methods aim to investigate whole-brain structural and functional changes in relation to aging. The analysis involves Functional and GM data from the ABCD dataset. For FCP components 2 and 4, there is a widespread association between their loadings and voxel-wise GM. Furthermore, there is evidence of connections between FCP and SCP loadings for certain components, suggesting that multivariate patterns of functional network connectivity (FNC) and gray matter (GM) exhibit associations with increasing age. Additionally, a gender-based analysis reveals differences

in SCP changes, with males showing less significant changes in SCP for component 2 and females displaying less significant SCP changes for component 1. These methods expand our understanding of age-related structural and functional brain changes, especially in the context of gender differences.

I will vary the component number to observe is there more stronger coupling between different brain region in increased component. I will also try to compute correlation between loading parameters and variable of interests.

REFERENCES

Abrol, A., Rashid, B., Rachakonda, S., Damaraju, E., & Calhoun, V. D. 2017, Frontiers in neuroscience, 11, 624

Andrews-Hanna, J. R., Snyder, A. Z., Vincent, J. L., Lustig, C., Head, D., Raichle, M. E., & Buckner, R. L. 2007, Neuron, 56, 924

Bandettini, P. A., Wong, E. C., Hinks, R. S., Tikofsky, R. S., & Hyde, J. S. 1992, Magnetic resonance in medicine, 25, 390

Beckmann, C. F., & Smith, S. M. 2005, Neuroimage, 25, 294

Bell, A. J., & Sejnowski, T. J. 1995, Neural computation, 7, 1129

Betzel, R. F., Byrge, L., He, Y., Goñi, J., Zuo, X.-N., & Sporns, O. 2014, Neuroimage, 102, 345

Bishop, C. M. 1999

Buxton, R. B., Wong, E. C., & Frank, L. R. 1998, Magnetic resonance in medicine, 39, 855

Calhoun, V., Adali, T., & Liu, J. 2006a, in 2006 International Conference of the IEEE Engineering in Medicine and Biology Society, IEEE, 3672–3675

Calhoun, V. D., Adali, T., Giuliani, N., Pekar, J., Kiehl, K., & Pearlson, G. 2006b, Human brain mapping, 27, 47

Calhoun, V. D., Miller, R., Pearlson, G., & Adalı, T. 2014, Neuron, 84, 262

Calhoun, V. D., & Sui, J. 2016, Biological psychiatry: cognitive neuroscience and neuroimaging, 1, 230

Calhoun, V. D., Wu, L., Kiehl, K. A., Eichele, T., & Pearlson, G. D. 2010, Acta neuropsychiatrica, 22, 127

Camara, E., Rodriguez-Fornells, A., & Münte, T. F. 2010, Journal of Neuroscience, 30, 11398

Caprihan, A., Pearlson, G. D., & Calhoun, V. D. 2008, Neuroimage, 42, 675

Chalfie, M., Sulston, J. E., White, J. G., Southgate, E., Thomson, J. N., & Brenner, S. 1985, Journal of Neuroscience, 5, 956

Chang, C., & Glover, G. H. 2010, Neuroimage, 50, 81

Chen, G. et al. 2011, Radiology, 259, 213

Choi, K., Yang, Z., Hu, X., & Mayberg, H. 2008, Psychiatric MRI/MRS, 16, 3

Correa, N. M., Adali, T., Li, Y.-O., & Calhoun, V. D. 2010a, IEEE signal processing magazine, 27, 39

Correa, N. M., Eichele, T., Adalı, T., Li, Y.-O., & Calhoun, V. D. 2010b, Neuroimage, 50, 1438

Correa, N. M., Li, Y.-O., Adali, T., & Calhoun, V. D. 2008, IEEE journal of selected topics in signal processing, 2, 998

Davis, T. L., Kwong, K. K., Weisskoff, R. M., & Rosen, B. R. 1998, Proceedings of the National Academy of Sciences, 95, 1834

DeRamus, T. et al. 2021, in 2021 IEEE 21st International Conference on Bioinformatics and Bioengineering (BIBE), IEEE, 1–6

Du, Y. et al. 2020, NeuroImage: Clinical, 28, 102375

Eichele, T., Calhoun, V. D., & Debener, S. 2009, International Journal of Psychophysiology,

73, 53

Fair, D. A., Cohen, A. L., Power, J. D., Dosenbach, N. U., Church, J. A., Miezin, F. M., Schlaggar, B. L., & Petersen, S. E. 2009, PLoS computational biology, 5, e1000381

Farras-Permanyer, L., Mancho-Fora, N., Montalà-Flaquer, M., Bartrés-Faz, D., Vaqué-Alcázar, L., Peró-Cebollero, M., & Guàrdia-Olmos, J. 2019, Neural regeneration research, 14, 1544

Fjell, A. M., Sneve, M. H., Grydeland, H., Storsve, A. B., Amlien, I. K., Yendiki, A., & Walhovd, K. B. 2017a, Human brain mapping, 38, 561

Fjell, A. M., Sneve, M. H., Grydeland, H., Storsve, A. B., & Walhovd, K. B. 2017b, Cerebral cortex, 27, 2303

Fox, M. D., & Raichle, M. E. 2007, Nature reviews neuroscience, 8, 700

Franco, A. R., Ling, J., Caprihan, A., Calhoun, V. D., Jung, R. E., Heileman, G. L., & Mayer, A. R. 2008, IEEE journal of selected topics in signal processing, 2, 986

Friston, K. J., Frith, C. D., Liddle, P. F., & Frackowiak, R. S. 1993, Journal of Cerebral Blood Flow & Metabolism, 13, 5

Geerligs, L., Renken, R. J., Saliasi, E., Maurits, N. M., & Lorist, M. M. 2015, Cerebral cortex, 25, 1987

Gray, J. M., Hill, J. J., & Bargmann, C. I. 2005, Proceedings of the National Academy of Sciences, 102, 3184

Greicius, M. D., Supekar, K., Menon, V., & Dougherty, R. F. 2009, Cerebral cortex, 19, 72

Groves, A. R., Beckmann, C. F., Smith, S. M., & Woolrich, M. W. 2011, Neuroimage, 54,

2198

Horn, A., Ostwald, D., Reisert, M., & Blankenburg, F. 2014, Neuroimage, 102, 142

Jafri, M. J., Pearlson, G. D., Stevens, M., & Calhoun, V. D. 2008, Neuroimage, 39, 1666

Jagannathan, K. et al. 2010, Biological psychiatry, 68, 657

Jorge, J., Van der Zwaag, W., & Figueiredo, P. 2014, Neuroimage, 102, 24

Kelly, A. C. et al. 2009, Cerebral cortex, 19, 640

Kim, D. I. et al. 2010, Neuroinformatics, 8, 213

Kim, S.-G., Jung, W. H., Kim, S. N., Jang, J. H., & Kwon, J. S. 2015, PLoS One, 10, e0127118

Krol, A., & Gimi, B. S. 2020, in Proc. of SPIE Vol, Vol. 11317, 1131701–1

Kwong, K. K. et al. 1992, Proceedings of the National Academy of Sciences, 89, 5675

Li, Y.-O., Adali, T., Wang, W., & Calhoun, V. D. 2009, IEEE Transactions on Signal Processing, 57, 3918

Liu, J., Bixler, J. N., & Calhoun, V. D. 2008a, in 2008 IEEE International Conference on Bioinformatics and Biomeidcine Workshops, IEEE, 151–157

Liu, J., & Calhoun, V. 2007, in 2007 4th IEEE International Symposium on Biomedical Imaging: From Nano to Macro, IEEE, 1028–1031

Liu, J., Pearlson, G., Windemuth, A., Ruano, G., Perrone-Bizzozero, N. I., & Calhoun, V. 2009, Human brain mapping, 30, 241

Liu, J., Xu, L., Caprihana, A., & Calhoun, V. D. 2008b, in 2008 IEEE International Conference on Acoustics, Speech and Signal Processing, IEEE, 449–452

Ogawa, S., Lee, T.-M., Kay, A. R., & Tank, D. W. 1990, proceedings of the National Academy of Sciences, 87, 9868

Oja, E., & Hyvarinen, A. 2000, Neural networks, 13, 411

Ouyang, X., Chen, K., Yao, L., Hu, B., Wu, X., Ye, Q., & Guo, X. 2015, Neuroscience, 301, 553

Radua, J., Canales-Rodríguez, E. J., Pomarol-Clotet, E., & Salvador, R. 2014, Neuroimage, 86, 81

Rykhlevskaia, E., Gratton, G., & Fabiani, M. 2008, Psychophysiology, 45, 173

Saha, D. K., Abrol, A., Damaraju, E., Rashid, B., Plis, S. M., & Calhoun, V. D. 2019, in 2019 IEEE 16th International Symposium on Biomedical Imaging (ISBI 2019), IEEE, 1602–1605

Saha, D. K., Damaraju, E., Rashid, B., Abrol, A., Plis, S. M., & Calhoun, V. D. 2020, bioRxiv, 2020

Saha, R., Saha, D. K., Rahaman, M. A., Fu, Z., & Calhoun, V. D. 2022, in 2022 IEEE 19th International Symposium on Biomedical Imaging (ISBI), IEEE, 1–4

Skudlarski, P., Jagannathan, K., Anderson, K., Stevens, M. C., Calhoun, V. D., Skudlarska, B. A., & Pearlson, G. 2010, Biological psychiatry, 68, 61

Specht, K., Zahn, R., Willmes, K., Krause, B., Herzog, H., & Huber, W. 2008, in Oral presentation on 14th Annual Meeting of the Organization of Human Brain Mapping, 14–19

Stevens, M. C. 2016, Neuroscience & Biobehavioral Reviews, 70, 13

Sui, J., Adali, T., Pearlson, G. D., & Calhoun, V. D. 2009a, Neuroimage, 46, 73

Sui, J., Adali, T., Pearlson, G. D., Clark, V. P., & Calhoun, V. D. 2009b, Human brain mapping, 30, 2953

Sui, J. et al. 2013, NeuroImage, 66, 119

Sui, J., Huster, R., Yu, Q., Segall, J. M., & Calhoun, V. D. 2014, Neuroimage, 102, 11

Sui, J., Pearlson, G., Caprihan, A., Adali, T., Kiehl, K. A., Liu, J., Yamamoto, J., & Calhoun, V. D. 2011, Neuroimage, 57, 839

Supekar, K., Musen, M., & Menon, V. 2009, PLoS biology, 7, e1000157

Teipel, S. J. et al. 2010, Neuroimage, 49, 2021

Thomason, M. E., Chang, C. E., Glover, G. H., Gabrieli, J. D., Greicius, M. D., & Gotlib, I. H. 2008, Neuroimage, 41, 1493

Tsang, A., Lebel, C. A., Bray, S. L., Goodyear, B. G., Hafeez, M., Sotero, R. C., McCreary, C. R., & Frayne, R. 2017, Frontiers in aging neuroscience, 144

Uludağ, K., & Roebroeck, A. 2014, Neuroimage, 102, 3

Váša, F. et al. 2020, Proceedings of the National Academy of Sciences, 117, 3248

——. 2018, Cerebral Cortex, 28, 281

Vértes, P. E., & Bullmore, E. T. 2015, Journal of Child Psychology and Psychiatry, 56, 299

Whitaker, K. J. et al. 2016, Proceedings of the National Academy of Sciences, 113, 9105

Xu, L., Pearlson, G., & Calhoun, V. D. 2009, Neuroimage, 44, 777

Zhang, D., Wang, Y., Zhou, L., Yuan, H., Shen, D., Initiative, A. D. N., et al. 2011, Neuroimage, 55, 856

Zhou, Y. et al. 2008, Schizophrenia research, 100, 120

Zhu, D. et al. 2014, NeuroImage, 102, 184

Zimmermann, J., Ritter, P., Shen, K., Rothmeier, S., Schirner, M., & McIntosh, A. R. 2016, Human brain mapping, 37, 2645